

# Speciation of Iron in Lithium Iron Phosphate (LFP) Cathode Material by LC-ICP-MS

Analysis of ferric ( $\text{Fe}^{3+}$ ) and ferrous ( $\text{Fe}^{2+}$ ) iron in lithium-ion battery cathode by Agilent 1260 Infinity II LC coupled to an Agilent 7850 ICP-MS

## Authors

Zhe Yan, Yingping Ni,  
Xiangcheng Zeng  
Agilent Technologies (China) Co. Ltd.,  
Shanghai, China



## Introduction

Lithium-ion batteries (LIBs) are often defined according to the material used for the cathode, since cathode composition influences the overall performance of the battery. LIB cathodes typically consist of lithium (Li) combined with a transition metal oxide that often includes cobalt (Co) as a major component. Examples of Co-based cathode compounds include Li Co oxide (LCO), nickel (Ni) manganese (Mn) Co oxide (NMC or NCM), Ni Co aluminum (Al) oxide (NCA), and Ni Mn Co Al oxide (NMCA).

Demand for LIBs is predicted to increase into the foreseeable future, but there are growing concerns associated with the mining, extraction, and use of the materials used in battery components, including Co-containing compounds. Co is a relatively rare element produced mainly as a by-product of copper or nickel mining, with most (~70%) coming from the Democratic Republic of Congo (DRC).

Around a quarter of the Co from the DRC is produced in artisanal mines, which are often unregulated and lack health and safety provision. Cobalt extraction also negatively impacts the environment, causing severe pollution around mining areas, especially in regions where compliance with environmental protection standards is poor. With only a few major sources of Co worldwide, the price can fluctuate, causing cost uncertainties for battery manufacturers. These factors have prompted many major battery producers to actively seek alternative, Co-free materials for their batteries.

Among alternative cathode materials, lithium iron phosphate (LFP) is one of the most interesting due to its relatively low cost, widespread availability of the raw materials, and fewer environmental and ethical concerns about accessing and extracting the elements. LFP also offers excellent thermal stability, good safety, long cycle life, and good performance at high temperatures, properties that are driving the increased use of LFP-LIBs in electric vehicles (1).

Trivalent or ferric iron (Fe(III), Fe<sup>3+</sup>) is considered an impurity in LFP cathode materials as it causes an increase in the self-discharge of the cathode and a decrease in the specific capacity. Controlling the Fe<sup>3+</sup> content is therefore one of the most important factors to ensure the quality of battery-grade LFP.

Currently, a titration method is typically used to determine total iron and Fe<sup>2+</sup> in LFP. However, the method is complex, requires large amounts of chemicals, and is time consuming (2–4). Capillary electrophoresis (CE) has been used to study the oxidation state of iron in LFP, using the complexation of Fe<sup>2+</sup> with 1,10-phenanthroline (*o*-phenanthroline) and Fe<sup>3+</sup> with ethylenediaminetetraacetic acid (EDTA) (5). The CE method requires the addition of a buffer solution during sample testing to prevent the complexation of *o*-phenanthroline and Fe<sup>3+</sup>.

Liquid chromatography (LC) equipped with an ion exchange column is widely used for the analysis of valence or oxidation states of various elements. LC is easily coupled to ICP-MS (LC-ICP-MS) to provide a sensitive, multi-elemental analytical technique for the detection and quantification of separated elemental species. LC-ICP-MS has been shown to be effective for separating Fe<sup>2+</sup> and Fe<sup>3+</sup> in environmental samples (6) and the technique might offer a useful alternative to existing techniques used for Fe speciation in LFP.

In this study, an analytical method was developed to measure the different valence states of iron in LFP using an Agilent LC-ICP-MS system. The method was evaluated for its suitability for the determination of the Fe<sup>3+</sup> impurity in LIB cathode materials.

## Experimental

### Reagents

Two LFP samples were bought from a commercial supplier of materials for the LIB industry. Ammonium ferrous sulfate hexahydrate ((NH<sub>4</sub>)<sub>2</sub>Fe(SO<sub>4</sub>)<sub>2</sub>(H<sub>2</sub>O)<sub>6</sub>) and pyridine-2,6-dicarboxylic acid (PDCA, C<sub>7</sub>H<sub>5</sub>NO<sub>4</sub>) were bought from Sigma-Aldrich. A 10,000 mg/L ferric iron standard solution (part number: 5190-8402) and tuning solution containing Li, Co, Y, Ce, Tl (p/n: 5188-6564) were obtained from Agilent. Ascorbic acid (C<sub>6</sub>H<sub>8</sub>O<sub>6</sub>) was bought from the China National Pharmaceutical Group Chemical Reagent Co., and ammonium nitrate (NH<sub>4</sub>NO<sub>3</sub>) was bought from J&K Scientific.

### Calibration standards

The 10,000 mg/L ferric iron standard solution was first diluted to give an intermediate stock at 500 mg/L. The ammonium ferrous sulfate hexahydrate was diluted to give an intermediate stock at 2000 mg/L as Fe(II). These two intermediate stocks were then used to prepare the calibration standards at the required concentrations in 2 nM ascorbic acid and 0.1% HCl. Calibration standard solutions were prepared at 0, 2.5, 5, 10, 20 mg/L for Fe(III) and 10x higher (0, 25, 50, 100, 200 mg/L) for Fe(II).

### Sample preparation

About 0.3 g of each LFP sample was accurately weighed into a 50 mL polypropylene bottle followed by 10% (v/v) hydrochloric acid (HCl) to a volume of 30 mL. The mixture was ultrasonicated at 60 °C for 30 minutes. The solution was filtered through a 0.22 μm filter membrane. To prepare the sample for analysis by LC-ICP-MS, 0.5 mL of the filtrate was diluted to 10 mL by adding 0.1% HCl and 2 nM ascorbic acid. The sample preparation therefore applied a total dilution factor of 2000x. The samples were transferred to amber vials (Agilent p/n 5183-4323) which had been cleaned with de-ionized water before use.

### Instrumentation

For the determination of the iron species in LFP, an Agilent 1260 Infinity II LC System was coupled to an Agilent ICP-MS using the Agilent LC Connection Kit. Integrated LC-ICP-MS system control and data processing was provided by the optional Plasma Chromatographic software module for Agilent ICP-MS MassHunter. In this work, an Agilent 7850 ICP-MS was used, but the method could also be run on the Agilent 7900 ICP-MS, which offers higher sensitivity and lower detection limits (DLs). The 1260 LC was equipped with a quaternary pump (p/n G7111B) and vial sampler (p/n G7129A). The LC was fitted with an Agilent Bio SAX ion exchange column (NP10, 4.6 x 250 mm, p/n 5190-2475) and

the LC column outlet was connected directly to the standard MicroMist nebulizer of the ICP-MS. For trace iron speciation applications, a bioinert LC would be recommended to minimize the Fe background signal from the stainless-steel components of the standard HPLC. But the concentration of iron in LFP is relatively high, so a small contribution from the Fe background signal does not affect the ability of the system to meet the analytical requirements for Fe speciation in LFP.

Agilent ICP-MS systems include the fourth generation Octopole Reaction System (ORS<sup>4</sup>) collision/reaction cell, which is optimized for control of common spectral interferences using helium cell gas and kinetic energy discrimination (He KED). The ICP-MS plasma conditions were optimized in He KED mode, so that the oxide ratio of CeO<sup>+</sup>/Ce<sup>+</sup> was less than 0.005 (0.5%). The ion lens voltages were automatically optimized to maximize sensitivity for the elements in the tuning solution by selecting “autotune” in the ICP-MS MassHunter software.

The LC-ICP-MS method was used to separate the two Fe species at room temperature using the operating conditions shown in Table 1. Peak integration was performed using the automatic integrator feature of the ICP-MS MassHunter Plasma Chromatographic software, which was used to control the coupled system and process the chromatographic data.

### Optimization of mobile phase and pH

The Bio SAX ion exchange column has a wide pH tolerance range of 2 to 12. However, a low mobile phase pH will lead to shorter column lifetime, as the mobile phase would be less effective to neutralize the acidic samples. The complexation (and therefore mobility) of ferrous iron with PDCA changes with pH (7), so pH can be used to control the retention time and resolution of Fe(III) from Fe(II).

**Table 1.** LC-ICP-MS operating conditions.

ICP-MS parameters	
RF Power (W)	1550
Sample Depth (mm)	10.0
Nebulizer Gas Flow (L/min)	0.75
Dilution Gas (L/min)	0.3
He Cell Gas Flow Rate (mL/min)	5
KED (V)	5
1260 HPLC parameters	
Mobile Phase	4 mM pyridine-2,6-dicarboxylic acid, 20 mM ammonium nitrate. pH adjusted to 5 with ammonia
Mobile Phase Flow Rate (L/min)	0.8
Injection Volume (μL)	30

The two iron species are separated more readily at a low pH. But if the pH is too low (or high), the retention times increase significantly and the Fe peaks may split, so four peaks appear. An optimized pH is also required to prevent the precipitation of Fe(III) (5). Lower pH favors the formation of only the Fe<sup>2+</sup> complex, and higher pH causes difficulty in eluting both Fe<sup>2+</sup> and Fe<sup>3+</sup> from the column (8). Therefore, to ensure good peak separation and maximize the life of the column, a mobile phase pH of 5 was selected. The pH was adjusted by the addition of ammonia.

As well as pH, the effect of altering the concentration of PDCA and ammonium nitrate in the mobile phase was investigated. Examples of three sets of method optimization conditions are shown by the overlaid chromatograms in Figure 1. The mobile phase composition that gave optimum peak shape, peak separation, and retention times is shown in purple (4 mM PDCA, 20 mM NH<sub>4</sub>NO<sub>3</sub>).

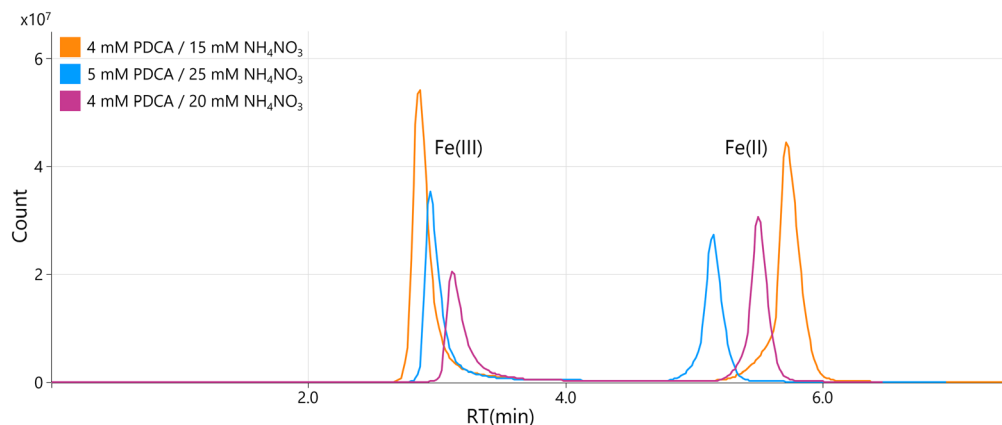


**Figure 1.** Overlaid chromatograms showing the effect of different concentrations of the mobile phase components and pH on the retention time and peak shape of Fe(III) and Fe(II).

## Results and discussion

The mixed Fe species standards were analyzed by LC-ICP-MS to create calibration curves for the two Fe species, as shown in Figure 2. Good linearity was achieved as shown by the correlation coefficients, which were better than 0.9996.

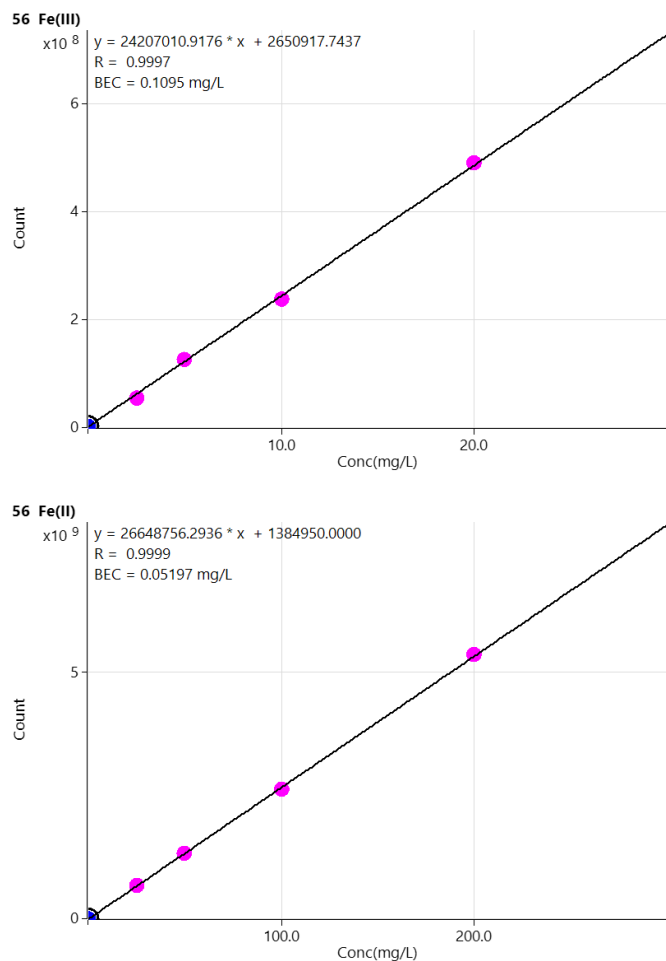


**Figure 2.** Calibration curves for ferric iron (top) and ferrous iron (bottom). Note that the Fe(II) standards are at 10x higher concentration levels than the Fe(III) standards.

## Sample analysis

The LC-ICP-MS method was used to determine the concentrations of Fe(III) and Fe(II) in two LFP samples, A and B, and the results are shown in Table 2. The total iron concentration, calculated from the sum of Fe(III) + Fe(II), is also shown. For comparison purposes and to verify the accuracy of the LC-ICP-MS method, total Fe was also determined in the LFP samples using a standard ICP-OES method. The LC-ICP-MS results for total iron (shown in Table 2) were within 2% of the results obtained using the established ICP-OES method, confirming the accuracy of the LC-ICP-MS method.

**Table 2.** Iron speciation and total iron concentrations determined by LC-ICP-MS and comparison to total iron results by ICP-OES.

LFP Sample	Iron Speciation Results (mg/kg)		Total Iron Results	
	Ferric Iron (Fe(III)) Concentration	Ferrous Iron (Fe(II)) Concentration	Sum of Fe(III) and Fe(II) by LC-ICP-MS (mg/kg)	Variation between LC-ICP-MS and ICP-OES results (%)
A #1	5195	340,472	345,668	-0.04
A #2	5104	342,431	347,535	1.51
A #3	4976	341,779	346,755	0.13
B #1	3980	341,429	345,409	0.94
B #2	3879	342,076	345,955	0.24
B #3	3875	337,065	340,940	0.56

## Spike recovery test

Because the iron concentration in the LFP sample solutions was high, it would have been difficult to spike iron into the undiluted sample at a high enough level for a spike recovery test. So, Fe(III) was spiked at 2 mg/L into the diluted LFP sample B after sample preparation. Due to the high concentration of ferrous iron in LFP, the prepared sample B was further diluted by a factor of about four before being spiked with Fe(II) at 50 mg/L. Duplicate spikes were prepared for both Fe species. As shown in Table 3, accurate spike recoveries of 100 ± 10% were obtained.

**Table 3.** Agilent LC-ICP-MS spike recovery results for ferric and ferrous iron in diluted LFP sample B. Spike levels were 2 mg/L for Fe(III) and 50 mg/L for Fe(II).

Iron Species	Unspiked LFP Sample (mg/L)	Spiked LFP Sample (mg/L)	Spike Recovery (%)
Fe(III)	2.09	3.91	91.4
		3.93	92.2
Fe(II)	36.45	83.95	95.0
		87.05	101.2

### Precision test

The precision of the method was checked by analyzing 13 separate solutions of LFP sample A by LC-ICP-MS. The 13 subsamples were prepared together to ensure that any oxidation effects were similar across all samples.

The overlaid chromatograms for all 13 sample injections are shown in Figure 3. For clarity, the chromatograms are displayed with different intensity scales for the intense Fe(II) peak (top) and the much less intense Fe(III) peak (bottom). For both forms of Fe, the overlay was nearly perfect, as confirmed by the low RSD for the peak height and peak area, shown in Table 4. The retention time stability was also excellent, with no variation between the 13 injections (SD of 0.0 min). The precision test results show that the method can reliably determine the concentrations of both ferrous iron and ferric iron in LFP in a single LC-ICP-MS measurement.

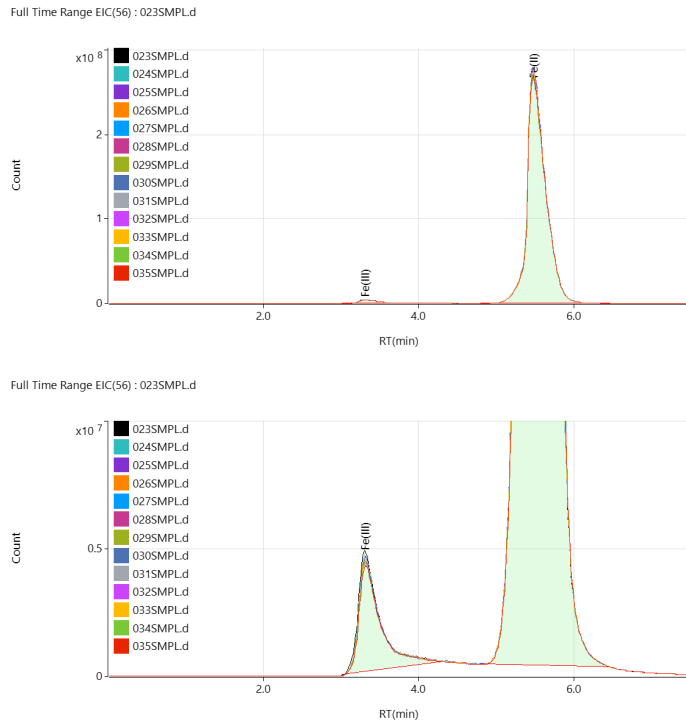


**Figure 3.** Top. Overlay of chromatograms of 13 subsamples of LFP sample A acquired by LC-ICP-MS, showing excellent reproducibility. Bottom. Same overlaid chromatograms with the intensity scale zoomed to show the good reproducibility of the much lower Fe(III) peak.

**Table 4.** Repeatability of peak height, peak area, and retention time for Fe(III) and Fe(II) in 13 subsamples of LFP sample A.

	Fe(III)		Fe(II)	
	Count/RT	RSD (%)	Count/RT	RSD (%)
Peak Height (count)	3996685	2.6	252431510	1.2
Peak Area (count)	76078424	1.6	4453923238	0.8
RT (min)	3.318	0.0*	5.485	0.0*

\* For both Fe species, the RT values were the same for all 13 replicate injections.

Table 5 shows the dilution-corrected concentration results for Fe(III) and Fe(II) in each of the 13 replicate samples, again indicating excellent reproducibility for the 13 separate analyses. The %RSDs were less than 2% for Fe(III) and less than 1% for Fe(II), demonstrating the robustness, stability, and repeatability of the method.

**Table 5.** Concentration results of Fe(III) and Fe(II) measured in 13 subsamples of LFP sample A. The data has been corrected for dilution.

LFP Sample A Replicate	Ferric Iron Concentration (mg/kg)	Ferrous Iron Concentration (mg/kg)
1	6,109	333,111
2	6,087	334,463
3	5,983	336,903
4	6,054	336,212
5	6,014	332,303
6	6,189	332,918
7	6,200	331,011
8	6,117	334,957
9	6,084	337,447
10	5,928	330,413
11	5,901	335,362
12	5,898	329,159
13	6,141	331,213
Average	6,055	333,498
RSD (%)	1.7	0.8

## Conclusion

As part of the drive to develop LIBs with improved performance, the battery industry is developing accurate methods to quality control the component parts of the batteries, especially materials used in the cathode, anode, and electrolyte. As well as monitoring other elemental contaminants, manufacturers need to determine the valence state of iron in the LFP cathode material. The level of Fe(III) (ferric iron) is an important quality indicator since Fe(III) is considered to be a contaminant in the LFP cathode material, which should contain mainly ferrous iron (Fe(II)). The separation and quantification of Fe(III) and Fe(II) in LFP was successfully carried out using an Agilent 1260 Infinity II LC fitted with an Agilent Bio SAX column coupled to an Agilent ICP-MS.

Compared with the more traditional test methods used for the determination of the different valence states of iron, the Agilent LC-ICP-MS method used simple pretreatment of the LFP sample. The total iron results for LFP, which were obtained by adding the concentration of Fe(III) and Fe(II) determined by LC-ICP-MS, were in good agreement with total iron levels determined by ICP-OES. The LC-ICP-MS method also demonstrated excellent precision and stability, with %RSDs below 2% for the measurement of both iron species in 13 subsamples of LFP.

The Agilent LC-ICP-MS method provides the LIB industry with a robust solution for the accurate measurement of the concentration of both total iron and the ferric iron impurity in LFP. Also, the ICP-MS can easily be uncoupled from the LC and used as a standalone ICP-MS for non-speciated analysis of other trace element contaminants in LIB components.

## References

1. Crownhart, C., Meet the new batteries unlocking cheaper electric vehicles, MIT Tech Review, 2023, accessed November 2023, <https://www.technologyreview.com/2023/02/17/1068814/meet-the-new-batteries-unlocking-cheaper-electric-vehicles/>
2. Pohl, P., Prusisz, B., Redox speciation of iron in waters by resin-based column chromatography, *Trends Anal Chem*, **2006**, 25: 909–916
3. Pehkonen, S. Determination of the Oxidation States of Iron in Natural Waters. *Analyst*, **1995**, 120: 265–2663
4. Achterberg, E.P., Holland, T.W., Bowie, A.R., Mantoura, R.F.C., Worsfold, P.J. Determination of iron in seawater. *Anal. Chim. Acta*, **2001**, 442:1–14
5. Hanf, L., Diehl, M., Kemper, L-S., Winter, M., Nowak, S., Investigating the oxidation state of Fe from LiFePO<sub>4</sub>-based lithium ion battery cathodes via capillary electrophoresis. *Electrophoresis*, **2020**, 41:1549–1556
6. Spolaor, A., Vallelonga, P., Gabrieli, J., Cozzi, G., Boutron, C., Barbante, C., Determination of Fe<sup>2+</sup> and Fe<sup>3+</sup> species by FIA-CRC-ICP-MS in Antarctic ice samples. *J. Anal. At. Spectrom.*, **2012**, 27:310–317
7. Soga, T., Ross, G.A., Simultaneous determination of inorganic anions, organic acids and metal cations by capillary electrophoresis. *J. Chromatogr. A*, **1999**, 834: 65–71
8. Wolle, M. M., et al. Method development for the redox speciation analysis of iron by ion chromatography–inductively coupled plasma mass spectrometry and carryover assessment using isotopically labeled analyte analogues. *J. Chromatogr. A*, **2014**, 1347: 93–103

[www.agilent.com/chem/7900icpms](http://www.agilent.com/chem/7900icpms)

DE00430463

This information is subject to change without notice.

© Agilent Technologies, Inc. 2023  
Published in the USA, November 23, 2023  
5994-6947EN